

Journal of Mechanics of Materials and Structures

**STRAIN GRADIENT FRACTURE OF A MODE III CRACK
IN AN ELASTIC LAYER ON A SUBSTRATE**

Jine Li and Baolin Wang

Volume 13, No. 4

July 2018



STRAIN GRADIENT FRACTURE OF A MODE III CRACK IN AN ELASTIC LAYER ON A SUBSTRATE

JINE LI AND BAOLIN WANG

This paper studies the problem of a mode III crack in an elastic layer on a substrate under the framework of strain gradient elasticity theory. The effects of volumetric and surface strain gradient parameters on the crack tip asymptotic stress and crack shape are investigated. Due to strain gradient effect, the crack opening, the magnitude of the stress ahead of the crack tip, and the stress intensity factor are significantly higher than those in classical linear elastic fracture mechanics. More significantly, the direction of the stress ahead of the crack tip with strain gradient is opposite to that in the classical linear elastic fracture mechanics. The conventional linear elastic fracture mechanics results are recovered when the gradient parameter reduces to zero. The influence of the substrate on the fracture mechanics parameters is very significant when the strain gradient effect of the materials is considered.

1. Introduction

Continuum methods, being less computationally intensive, have been extensively used to investigate the macro structural behavior on theoretical as well as the empirical grounds. Classical continuum elasticity theories assume that the stresses in a material point depend only on the strain components at that point. They do not account for the contributions of strain gradients therefore can not account for size effects of materials, which are more evident when the dimensions of the structures are scaled down to the micro and nano-domains. In that case, the material microstructural length scales become comparable to the length scale of deformation field that tends to cause non-homogenous and scale/size dependent mechanical behavior [Giannakopoulos and Stamoulis 2007].

Size dependent mechanical behavior in micro-scale elements have been observed extensively in experiments [Fleck et al. 1994; Stolken 1997; Ma and Clarke 1995; McElhaney et al. 1998; Nix 1989; Poole et al. 1996; Stelmashenko et al. 1993]. Size dependence of the stiffness of the material was also confirmed by micro-cantilever experiments conducted by McFarland and Colton [2005]. It has been understood that the non-classical continuum theories such as the higher-order gradient theories and couple stress theory can interpret the scale-dependent behaviour of materials. Mindlin and Tiersten [1962], Toupin [1962], and Koiter [1964] introduced the couple stress elasticity theory, incorporating two higher order material constants to predict the size effects. The higher-order strain gradient theory was introduced by Mindlin [1965] that includes the effect of the first and second derivatives of the strain tensor on the strain energy density. Lam et al. [2003] introduced three higher-order material constants in the constitutive equations of the modified strain gradient theory. In several modern theories, the response at a certain scale is influence by a characteristic length at the lowest level [Benvenuti and Simone 2013]. This is very evident in the case of lattice system potential energy that depends on the inter-atomic distance [Kiang et al. 1998]. In

Keywords: Strain gradient elasticity, film-substrate structure, mode III crack, crack tip field, fracture mechanics.

order to cater for the underlying microstructure into the continuum theory, higher order strain gradient theories were presented by Mindlin and Eshel [1968].

On the other hand, strain gradient effects become important near a crack tip because of the strain singularity, particularly when the size of fracture process zone is on the order of the intrinsic material length. Over the years, a few studies related to a crack in an infinite medium were conducted based on gradient elasticity theories. The pioneering works are gradient elasticity with mode III cracking investigated by Vardoulakis et al. [1996], Exadaktylos et al. [1996], and subsequently by Exadaktylos [1998] for the mode I fracture and Exadaktylos and Vardoulakis [2001] for the scale related fracture in rock mechanics. In a series of excellent studies, Fannjiang et al. [2002], Paulino et al. [2003], and Chan et al. [2008] applied gradient elasticity theory to mode III crack problems in functionally graded materials for cracks perpendicular and parallel to the material gradation direction, respectively. Some interesting information related to dislocation based-gradient elastic fracture mechanics for the anti-plane crack problem is discussed by Mousavi and Aifantis [2005]. Karimipour and Fotuhi [2017] carried out a comprehensive study for an anti-plane infinite plane with multiple cracks. In a series of studies, Wu and his colleagues have explored the thermally induced fracture of interface crack in bi-material structures [Wu et al. 2016a], crack tip field and crack extension in functionally graded materials [Shi et al. 2014], and film/substrate structures with ferroelectric effect [Qiu et al. 2018; Wu et al. 2016b].

Furthermore, investigations of cracking of a surface layer on a substrate of different materials have its root application for ensuring the reliability of coating/substrate structures [Grosskreutz and Mcneilt 1969; Kim and Nairn 2000]. Fracture mechanics analysis of such problem has attracted interests from numerous researchers including world-class scientist in the field (e.g., Hutchinson et al. 1987; Schulze and Erdogan 1998). So far, fracture mechanics of strain gradient materials have been limited to an infinite medium so that the only length parameter is the crack size. Strain gradient fracture of layered composite materials, however, is very rare. Therefore, this paper investigates the problem of an anti-plane (mode III) crack in an elastic layer on a substrate. The crack opening displacements, the stress at the crack tip front and the stress intensity factors are shown graphically. Many observations different from those of the conventional linear elastic fracture mechanics are observed.

2. Anti-plane deformation with strain gradient effects

This paper considers a cracked strain gradient layer on a substrate of different material as shown in Figure 1. The crack has length $2a$ and is at the interface of two strain gradient layers of heights h_1 and h_2 , respectively. We consider the anti-plane problem such that the only non-vanishing displacement component is along the z axis and is denoted as w .

The constitutive equations and theoretical formulations for the anti-plane deformation of strain gradient materials are similar to those adopted by Vardoulakis et al. [1996] and Exadaktylos [1998]. There are two material length parameters that are responsible for material volumetric and surface strain gradient terms. These material constants are denoted as l and l' , respectively. This theory has been successfully employed to study the size effects in bending of micro-cantilever beams [Aifantis 2016], twisting of micro-wires [Aifantis 2011], and fracture [Giannakopoulos and Stamoulis 2007]. According to gradient elasticity theory, the stresses and double stresses derived from the constitutive equations of gradient elasticity with surface energy are given by the following equations (see [Chan et al. 2008; Paulino et al.

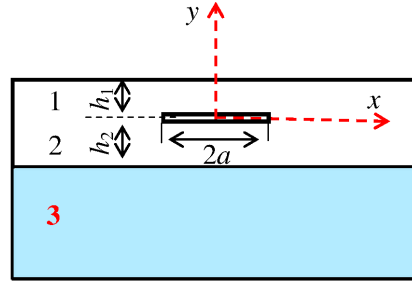


Figure 1. A crack in a strain gradient layer on a substrate: the strain gradient layer (1, 2) and the substrate (3).

2003; Vardoulakis et al. 1996], for example):

$$\tau_x = G \left[\frac{\partial w}{\partial x} - l^2 \nabla^2 \frac{\partial w}{\partial x} \right], \quad \tau_y = G \left[\frac{\partial w}{\partial y} - l^2 \nabla^2 \frac{\partial w}{\partial y} \right], \quad (1a)$$

$$\mu_{xx} = Gl^2 \frac{\partial^2 w}{\partial x^2}, \quad \mu_{xy} = Gl^2 \frac{\partial^2 w}{\partial x \partial y}, \quad (1b)$$

$$\mu_{yx} = G \left[-l' \frac{\partial w}{\partial x} + l^2 \frac{\partial^2 w}{\partial x \partial y} \right], \quad \mu_{yy} = G \left[-l' \frac{\partial w}{\partial y} + l^2 \frac{\partial^2 w}{\partial y^2} \right]. \quad (1c)$$

Here $\nabla^2 = \partial^2/\partial x^2 + \partial^2/\partial y^2$, l and l^2 are the volumetric and surface material characteristic lengths, respectively, G is the shear modulus, τ is the stress tensor, and μ is the double stress tensor, l and l^2 are characteristic material lengths related to volume and surface energy, respectively, restricted (in order for the strain energy density to be positive definite) such that $-1 < l'/l < 1$ [Exadaktylos et al. 1996; Vardoulakis et al. 1996]. This means that the surface length l' cannot exist alone (i.e. $l' \neq 0$ and $l = 0$ is not acceptable). When the surface energy l' is omitted, the closed form solution for an infinite medium with a crack has been obtained by Zhang et al. [1998].

The constitutive equations (1a) and (1b) show that the high order strains are considered however the high order stresses are ignored. The equilibrium equation remains the same as the classical one and is $\partial \tau_x/\partial x + \partial \tau_y/\partial y = 0$. This can be expressed in terms of the displacement component w with the help of (1a) as

$$\left[\frac{\partial^2 w}{\partial x^2} + \frac{\partial^2 w}{\partial y^2} \right] - l^2 \left[\frac{\partial^4 w}{\partial x^4} + 2 \frac{\partial^4 w}{\partial x^2 \partial y^2} + \frac{\partial^4 w}{\partial y^4} \right] = 0. \quad (2)$$

The general solution of the fourth order differential Equation (2) may be represented as $w(x, y) = w^c(x, y) + w^s(x, y)$, where w^c is the general solution of the harmonic equation $\partial^2 w/\partial x^2 + \partial^2 w/\partial y^2 = 0$ and w^s is a particular solution of (2). The application of Fourier transform gives the solution of harmonic equation as

$$w^c(x, y) = \frac{1}{2\pi} \int_{-\infty}^{\infty} [A(s) e^{-|s|y} + C(s) e^{|s|y}] e^{-isx} ds. \quad (3a)$$

A particular solution of (2) can be given as

$$w^g(x, y) = \frac{1}{2\pi} \int_{-\infty}^{\infty} [B(s) e^{-|s_1|y} + D(s) e^{|s_1|y}] e^{-isx} ds, \quad (3b)$$

where $|s_1| = \sqrt{s^2 + (1/l^2)}$. Combining (3a) and (3b) gives the general solution of (2):

$$w(x, y) = \frac{1}{2\pi} \int_{-\infty}^{\infty} [A(s) e^{-|s|y} + B(s) e^{-|s_1|y} + C(s) e^{|s|y} + D(s) e^{|s_1|y}] e^{-isx} ds. \quad (4)$$

The constants $A(s)$, $B(s)$, $C(s)$, and $D(s)$ are to be determined from the boundary conditions of the problem. For the purpose of the following analysis, the shear stress $\tau_y(x, y)$ obtained from (1b) and (4) is written as

$$\tau_y(x, y) = -\frac{G}{2\pi} \int_{-\infty}^{\infty} |s| [A(s) e^{-|s|y} - C(s) e^{|s|y}] e^{-isx} ds, \quad (5)$$

and the double stress $\mu_{yy}(x, y)$ obtained from (1c) and (4) is written as

$$\begin{aligned} \mu_{yy} = \frac{Gl'}{2\pi} \int_{-\infty}^{\infty} \left[|s|A(s) e^{-|s|y} + |s_1|B(s) e^{-|s_1|y} \right. \\ \left. - |s|C(s) e^{|s|y} - |s_1|D(s) e^{|s_1|y} \right] e^{-isx} ds \\ + \frac{Gl^2}{2\pi} \int_{-\infty}^{\infty} \left[A(s) e^{-|s|y} s^2 + B(s) e^{-|s_1|y} s_1^2 \right. \\ \left. - C(s) e^{|s|y} s^2 + D(s) e^{|s_1|y} s_1^2 \right] e^{-isx} ds. \quad (6) \end{aligned}$$

In the following analysis, we will use the subscripts 1, 2 and 3 to distinguish the regions $0 \leq y \leq h_1$, $-h_2 \leq y \leq 0$, and $y \leq -h_2$, respectively (see Figure 1). The crack is at the $y = 0$ plane and the interface of the structure is at the $y = -h_2$ plane. The displacement, stress and double stress of the substrate layer are, respectively

$$w_3(x, y) = \frac{1}{2\pi} \int_{-\infty}^{\infty} [C_3(s) e^{|s|y} + D_3(s) e^{|s_3|y}] e^{-isx} ds, \quad (7)$$

$$\tau_y(x, y) = \frac{G_s}{2\pi} \int_{-\infty}^{\infty} |s| C_3(s) e^{|s|y} e^{-isx} ds, \quad (8)$$

and

$$\begin{aligned} \mu_{3yy} = \frac{G_s l'_s}{2\pi} \int_{-\infty}^{\infty} [-|s|C_3(s) e^{|s|y} - |s_3|D_3(s) e^{|s_3|y}] e^{-isx} ds \\ + \frac{G_s l_s^2}{2\pi} \int_{-\infty}^{\infty} [C_3(s) e^{|s|y} s^2 + D_3(s) e^{|s_3|y} s_3^2] e^{-isx} ds, \quad (9) \end{aligned}$$

where $|s_3| = \sqrt{s^2 + (1/l_3^2)}$, and where l_3 is the strain gradient parameter of the substrate layer.

3. The crack problem and its solution

The stress free conditions on the top surface requires that $\tau_{1y}(x, h_1) = 0$ and $\mu_{1yy}(x, h_1) = 0$. The transmission conditions for ideal interface imply continuity of the stress, double stress, displacements and rotations [Piccolroaz et al. 2012]. Thus $\tau_{1y}(x, 0) = \tau_{2y}(x, 0)$, $\mu_{1yy}(x, 0) = \mu_{2yy}(x, 0)$, $\partial w_1(x, 0)/\partial y =$

$\partial w_2(x, 0)/\partial y$, $\tau_{2y}(x, -h_2) = \tau_{3y}(x, -h_2)$, $\mu_{2yy}(x, -h_2) = \mu_{3yy}(x, -h_2)$, $w_2(x, -h_2) = w_3(x, -h_2)$. These represent the continuity conditions of the displacement and stress at the bonded region of the interfaces. As usually in the fracture mechanics analysis, the crack surfaces are assumed to be subjected to an applied anti-plane shear stress $p(x)$ such that the following mixed boundary conditions on the $y = 0$ plane hold (these boundary conditions were obtained from the variational principle and have been used by Paulino et al. [2003] and Chan et al. [2008])

$$\tau_y(x, 0) = -p(x), \quad |x| < a, \tag{10a}$$

$$w_1(x, 0) - w_2(x, 0) = 0, \quad |x| \leq a. \tag{10b}$$

In order to determine the full-field solution of the problem, we also introduce a discontinuity function $g(x)$ along the cracked plane according to

$$g(x) = \frac{\partial[w_1(x, 0) - w_2(x, 0)]}{\partial x}. \tag{11}$$

By this definition, the continuity condition for the displacement on the $y = 0$ plane requires that $g(x) = 0$ for $|x| \geq a$ and $\int_{-a}^a g(x) dx = 0$, which is the single-value condition.

Substituting (4) into (11) and with Fourier inversion, a relationship between $A(s)$, $B(s)$, $C(s)$, and $D(s)$ can be obtained:

$$[A_1(s) + B_1(s) + C_1(s) + D_1(s)] - [A_2(s) + B_2(s) + C_2(s) + D_2(s)] = \frac{i}{2s} \int_{-a}^a g(r) e^{isr} dr. \tag{12}$$

As a result, $A_i(s)$, $B_i(s)$, $C_i(s)$ and $D_i(s)$ ($i = 1, 2, 3$) can be expressed in terms of the single unknown function $g(x)$. Suppose the expressions for $A_1(s)$ and $C_1(s)$ are, respectively,

$$A_1(s) = \bar{A}(s) \frac{i}{2s} \int_{-a}^a g(r) e^{isr} dr, \tag{13a}$$

and

$$C_1(s) = \bar{C}(s) \frac{i}{2s} \int_{-a}^a g(r) e^{isr} dr. \tag{13b}$$

Then the shear stress on the cracked obtained with the submission of (13a) and (13b) into (5) is

$$\tau_y(x, 0) = G_1 \int_{-a}^a R(x, r) g(r) dr, \tag{14}$$

where the integral kernel $R(x, r)$ is

$$R(x, r) = \lim_{y \rightarrow +0} \frac{i}{2\pi} \int_{-\infty}^{\infty} \frac{1}{2} \frac{|s|}{s} (-\bar{A}(s) e^{-|s|y} + \bar{C}(s) e^{|s|y}) e^{is(r-x)} ds, \tag{15}$$

or

$$R(x, r) = \lim_{y \rightarrow +0} \frac{1}{2\pi} \int_0^{\infty} (\bar{A}(s) e^{-|s|y} - \bar{C}(s) e^{|s|y}) \sin[s(r-x)] ds. \tag{16}$$

In order to identify the asymptotic behaviour of $\bar{A}(s) - \bar{C}(s)$ for s at infinity, one can consider a crack of length $2a$ at the infinite medium of the same material of the layer. This is, one considers h to be equal to infinity. After examining, it is found that for large values of s , $\bar{C}(s)$, and $\bar{D}(s)$ become

vanishing and $\bar{A}(s)$ approaches to $1 + l^2 s^2$. This function is denoted as $\Lambda_0(s)$ in the following analysis. The asymptotic analysis allowing splitting of the integral kernel $R(x, r)$ into two parts so that the stress of (14) can be re-written as

$$\tau_y(x, 0) = G \int_{-a}^a \Omega(x, r) g(r) dr + G \int_{-a}^a R_\infty(x, r) g(r) dr, \quad (17)$$

where the regular kernel is

$$\Omega(x, r) = \frac{1}{2\pi} \int_0^\infty (\bar{A}(s) - \bar{C}(s) - \Lambda_0(s)) \sin[s(r-x)] ds, \quad (18)$$

and the singular kernel is

$$R_\infty(x, r) = \frac{1}{2\pi} \int_0^\infty [1 + l^2 s^2] \sin[s(r-x)] ds. \quad (19)$$

The regular kernel, Equation (18) can be evaluated by standard numerical integral technique. The singular kernel, Equation (19) can be evaluated by hypersingular integral equation technique of Paulino et al. [2003] and Chan et al. [2008]. As a result of such procedure, we get

$$\tau_y(x, 0) = -\frac{Gl^2}{\pi} \int_{-a}^a \frac{g(r)}{(r-x)^3} dr + \frac{G}{2\pi} \int_{-a}^a \frac{g(r)}{r-x} dr + G \int_{-a}^a \Omega(x, r) g(r) dr. \quad (20)$$

Equation (20) provides the expression for $\tau_y(x, 0)$ outside as well as inside the crack. In the case of inside the crack, the crack face stress boundary condition gives

$$-\frac{(l/a)^2}{\pi} \int_{-1}^1 \frac{g(r)}{(\bar{r}-\bar{x})^3} d\bar{r} + \frac{1}{2\pi} \int_{-a}^a \frac{g(r)}{\bar{r}-\bar{x}} d\bar{r} + a \int_{-1}^1 \Omega(x, r) g(r) d\bar{r} = -\frac{P}{G}. \quad (21)$$

Here and in the following, the notations $\bar{x} = x/a$ and $\bar{r} = r/a$ will be used. Equation (21) is a hypersingular integral equation. According to Paulino et al. [2003] and Chan et al. [2008], the solution of $g(r)$ can be expressed in the following form:

$$g(\bar{r}) = \sum_{m=1}^{\infty} C_m U_m(\bar{r}) \sqrt{1-\bar{r}^2}, \quad (22)$$

in which U_m is the Chebyshev polynomial of the second kind $U_m(\bar{x}) = \sin[(m+1)\arccos(\bar{x})]/\sqrt{1-\bar{x}^2}$, and C_m are unknowns to be evaluated. It is observed that the single-value condition of $g(x)$ is identically satisfied by (22). After substituting (22), truncated with the first M terms, into (21), and following the same procedure of Paulino et al. [2003] and Chan et al. [2008], and through expansions and integrals of Chebyshev polynomials given in Appendix, it can be seen that

$$-\frac{(l/a)^2}{4(1-\bar{x}^2)} \sum_{m=1}^{\infty} C_m [m(m+1) U_{m+1}(\bar{x}) - (m^2 + 3m + 2) U_{m-1}(\bar{x})] - \frac{1}{2} \sum_{m=1}^{\infty} C_m T_{m+1}(\bar{x}) + a \sum_{m=1}^{\infty} C_m V_m(\bar{x}) = -\frac{P}{G}, \quad (23)$$

where T_m is the Chebyshev polynomial of the first kind $T_m(\bar{x}) = \cos[m \arccos(\bar{x})]$, and V_m is

$$V_m(\bar{x}) = \int_{-1}^1 \Omega(x, r) U_m(\bar{r}) \sqrt{1 - \bar{r}^2} d\bar{r}. \tag{24}$$

For the case of infinite layer thickness, the regular integral kernel $\Omega(x, r)$ vanishes and (23) becomes

$$-\frac{(l/a)^2}{4(1 - \bar{x}^2)} \sum_{m=1}^{\infty} C_m [m(m+1) U_{m+1}(\bar{x}) - (2m^2 + 3m + 2) U_{m-1}(\bar{x})] - \frac{1}{2} \sum_{m=1}^{\infty} C_m T_{m+1}(\bar{x}) = -\frac{P}{G}. \tag{25}$$

The simplest method for solving the functional (23) is using an appropriate collocation in x . After evaluating C_m from (23), the displacement field can be calculated from (4) since $A(s)$, $B(s)$, $C(s)$, and $D(s)$ have been expressed in terms of $g(x)$. The associated stress can be obtained from the constitutive equations of (1a)–(1c). Thus, the full field solution is obtained.

Of particular interest are the crack opening displacement and the crack tip stress state. The displacement jump across the crack can be evaluated from $\Delta w(x, 0) = \int_{-a}^x g(r) dr$. With the substitution of (27), we get

$$\Delta w(x, 0) = a \sum_{m=1}^M C_m \left(\frac{\sin[(m+2) \arccos(x/a)]}{2(m+2)} - \frac{\sin[m \arccos(x/a)]}{2m} \right), \quad |x| < a. \tag{26}$$

Due to symmetry, the displacement on the upper surface of the crack $w(x, 0)$ is half of $\Delta w(x, 0)$. The maximum cack face displacement appears at $x = 0$ on the upper surface of the crack and is

$$w(0, 0) = \frac{\Delta w(0, 0)}{2} = -a \sum_{m=1}^M C_m \frac{\sin(m \pi/2)}{4} \left(\frac{1}{m+2} + \frac{1}{m} \right).$$

For gradient elasticity theory, τ_y have a strong singularity, which can not be described by conventional linear elasticity fracture mechanics. Note that the expression for $\tau_y(x, 0)$ is valid for $|x| < a$ as well as $|x| > a$. Equation (20) provides the expression for $\tau_y(x, 0)$ outside as well as inside the crack. With the substitution of the density function (22) and again through expansions of Chebyshev polynomials [Chan et al. 2003], the stress near the crack tip is found to be (neglect the secondary terms)

$$\begin{aligned} \tau_y(x, 0) = & -\frac{G}{2} \sum_{m=1}^{\infty} C_m \left(\bar{x} - \frac{|x|}{x} \sqrt{\bar{x}^2 - 1} \right)^{m+1} + \frac{G(l/a)^2}{2} \sum_{m=1}^{\infty} C_m (m+1) \left(\bar{x} - \frac{|x|}{x} \sqrt{\bar{x}^2 - 1} \right)^{m-1} \\ & \times \left[m \left(1 - \frac{|\bar{x}|}{\sqrt{\bar{x}^2 - 1}} \right)^2 + \frac{\bar{x} - \frac{|x|}{x} \sqrt{\bar{x}^2 - 1}}{(\sqrt{\bar{x}^2 - 1})^3} \right]. \tag{27} \end{aligned}$$

The highest singularity is $(\bar{x} - 1)^{3/2}$. This is totally different from the conventional linear elasticity fracture mechanics result, which gives $(\bar{x} - 1)^{1/2}$ singularity.

The above formulation is general enough for consideration of a crack at any position in the film with or without substrate. For example, if we let $G_s = 0$, the problem will become a crack in a single layer. On the other hand, if we let $G_s = \infty$, the problem will correspond to a crack in a film on a rigid substrate. It can be seen that the value of l' does not appear in (21). Thus, the solution of the discontinuity function $g(x)$ has no dependence on the material gradient parameter l' which is related to the surface energy. One can

also see that the shear stress τ_y on the cracked plane also does not depend on l' . However, it is expected that the other stress components such as τ_x should have a dependence on l' . The stress component τ_y away from the cracked plane should also have relationship with l' . Karimipour and Fotuhi [2017] have also observed that the effect of the volumetric characteristic length l on the solution is more significant than that of the surface characteristic length l' and suggested that it is quite adequate if only the effect of l is studied.

4. Results and discussion

All results are given for the z direction displacement on the upper surface of the crack and the stress ahead of the crack tip on the cracked plane for a constant surface shear load $\tau_y(x, 0) = -p_0$ on the crack faces. It is noticed from the calculations that the value of M required for a convergent result depends on the relative value of strain gradient l to the crack length parameter a . All calculations confirm that the results converge as the number of allocation points (the value of M) increase.

In order to examine the influence of crack location, we consider a film on a substrate of the same material. This structure configuration can also be understood as a semi-infinite medium containing a crack at any location. Therefore, the effect of h_2 is dropped out from the result. Some numerical results of crack surface displacement profiles for various values of h_1 are shown in Figure 2 for $l = 0.2a$. The crack is considerably softened as it approaches the surface of the film. This fact can also be seen from Figure 3 which shows the influence of crack location on the stress ahead of the crack tip. As expected,

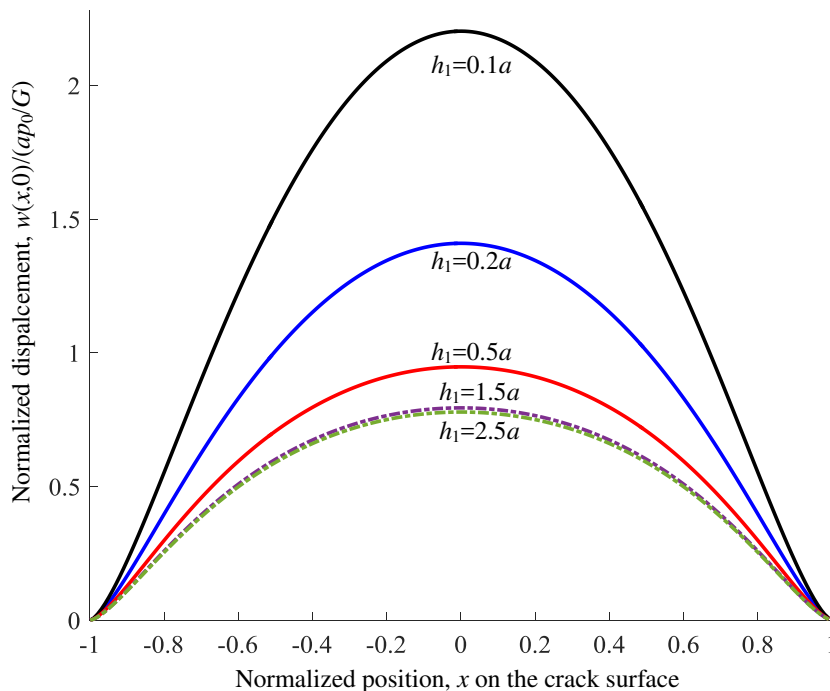


Figure 2. Crack surface displacement profiles for a film on the substrate of the same material with choice of $l = 0.2a$.

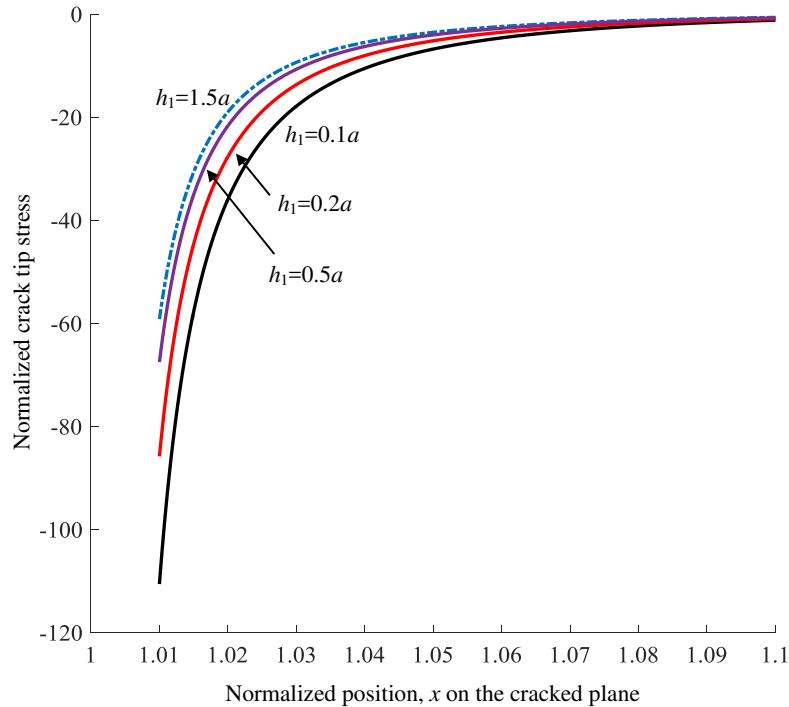


Figure 3. Normalized stress $\tau_y(x, 0)/p_0$ near the right crack tip for a film on the substrate of the same material with choice of $l = 0.2a$.

the stress is significantly enhanced when h_1 is smaller. Results for the value of h_1 larger than $1.5a$ are almost identical to those for a crack in an infinite medium. Basically, the effect of strain gradient on the crack in the finite layer is more significant than in the infinite layer. Generally, finite layer border tends to enhance the stress level near the crack tip.

Some numerical results for a crack at $h_1 = 0.2a$ in a film on a substrate of the same material is plotted in Figure 4 to show the effect of the gradient parameter l . It can be seen that the displacement decreases considerably with the gradient parameter. Therefore, in comparison to the classical elasticity fracture mechanics, strain gradient effect will considerably stiffens the crack. As observed, when the gradient parameter become very small (in current case, $l/a \leq 0.005$), the result is almost identical to the that obtained from the conventional linear elastic fracture mechanics analysis.

In order to further explore the strain gradient effect, it is necessary to know the stress near the crack tips and to evaluate the influence of the gradient parameter l . Therefore, in Figure 5, the normalized stresses near the right crack tip for a crack at $h_1 = 0.2a$ in a film on the substrate of the same material are plotted for different values of l . The stresses at the left crack tip are same but with an opposite sign. It is obvious from Figure 5 that the magnitudes of the stress increase as l/a increases and vice versa. This suggests that the stresses in strain gradient fracture are significantly larger than those in the classical field. This trend observation is the same as that made by Zhang et al. [1998] based on the closed-form analysis of an infinite medium with an anti-plane crack. Another fact observed from Figure 5 is that for sufficiently small gradient parameter, the strain gradient solution can be reduced to that of

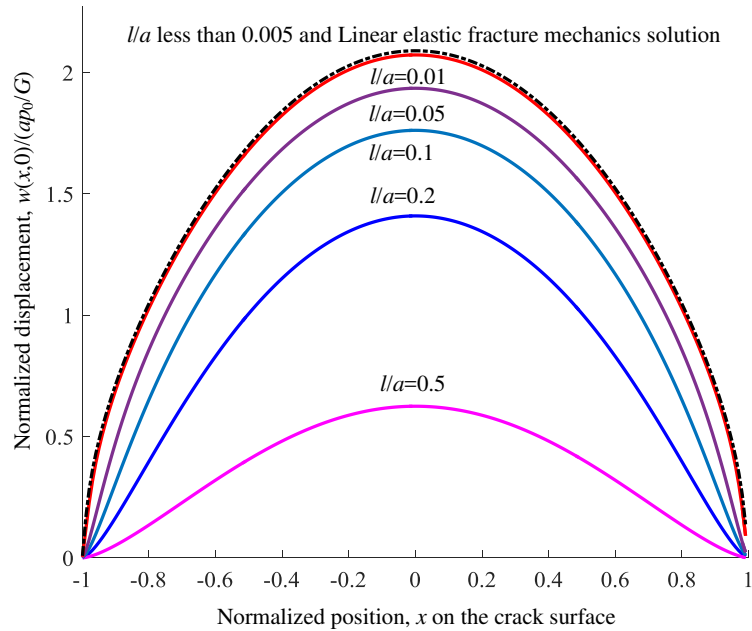


Figure 4. Crack (upper) surface displacement profiles for a crack at $h_1 = 0.2a$, in a film on the substrate of the same material for different values of l .

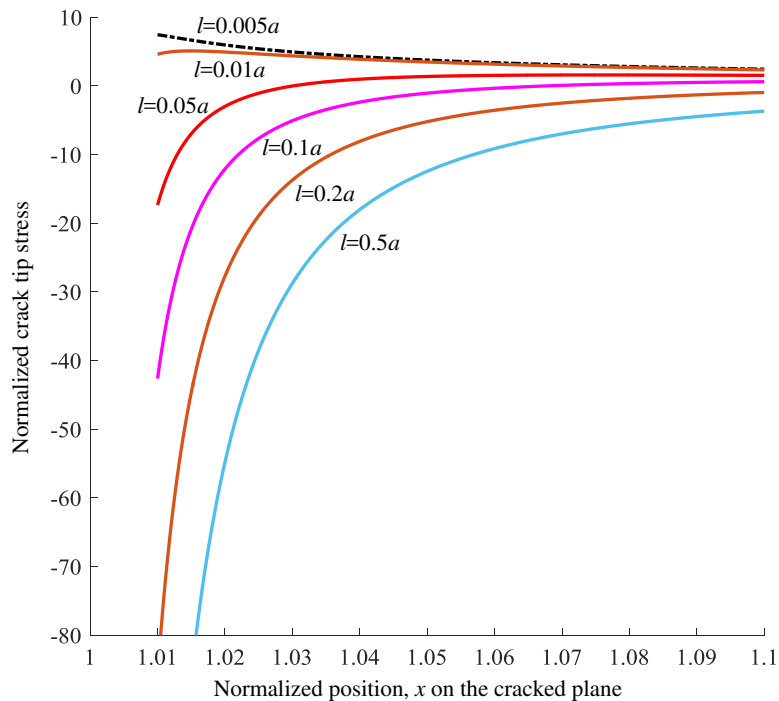


Figure 5. Normalized stress $\tau_y(x, 0)/p_0$ near the right crack tip for a crack at $h_1 = 0.2a$, in a film on the substrate of the same material for different values of l .

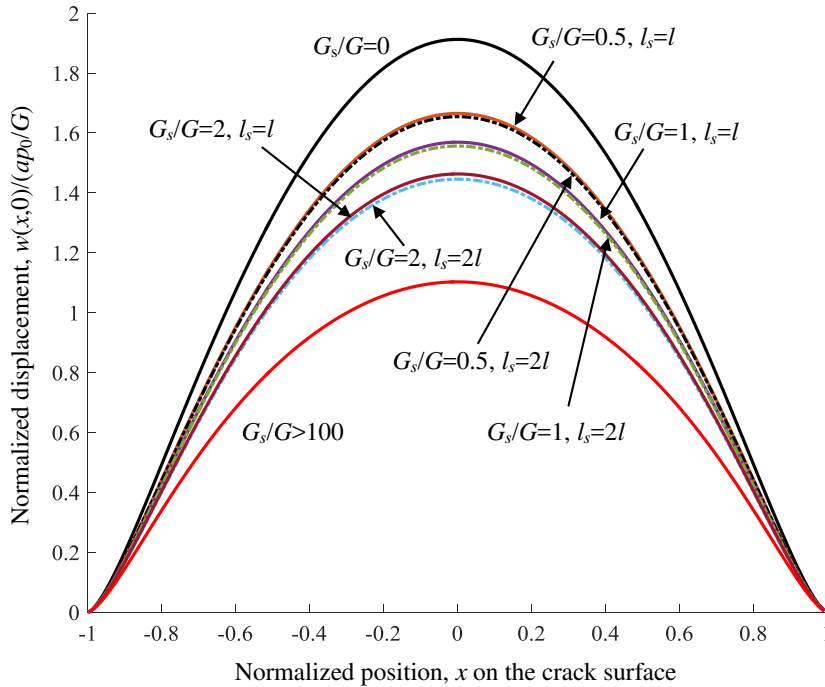


Figure 6. Crack surface displacement profiles in a film on a substrate of different stiffness and gradient parameter for $h_1 = h_2 = 0.2a$ and $l = 0.2a$.

the conventional linear elastic fracture mechanics solution. However, the natures of the strain gradient solution and the conventional linear elastic fracture mechanics solution are totally different: the gradient solutions are always negative and with a higher magnitude of the stress level but the conventional linear elastic fracture mechanics solution is always positive and with a lower magnitude of the stress level.

Figure 6 displays variation of the crack surface displacement with the stiffness of the substrate for a crack at the center of the film with $h_1 = h_2 = 0.2a$ and for $l = 0.2a$. As expected, the structure becomes stiffer and the crack surface displacement reduces when the shear modulus of the substrate layer increases. The zero substrate stiffness is related to a single layer with a crack. On the other hand, the infinite layer thickness corresponds to a single layer on a rigid substrate. From Figure 6 we can observe the influence of the gradient parameter of the substrate on the crack displacement. Generally, the gradient of the substrate reduces the crack face displacement. However, this effect is very small. Figure 7 shows variations of the stress at the right crack tip for $h_1 = h_2 = 0.2a$, $l = 0.2a$ and $l_s = 2l$. Apparently, the substrate provides a constraint to the film so that the crack tip stresses are reduced. The higher the value of the shear modulus of the substrate, the lower the crack tip stress. Since the influence of the gradient parameter of the substrate can not be observed when it is plotted in the figure, the results for other values of the substrate gradient parameters are not given in Figure 7.

Because the stresses are singular at the crack tips, it is necessary to study the intensity of the stress concentration near the crack front. For this, it is important to recognize that the stress at the crack tip has $(x^2 - a)^{-3/2}$ singularity when $x \rightarrow a^+$ or $x \rightarrow -a^-$. Paulino et al. [2003] defined the generalized

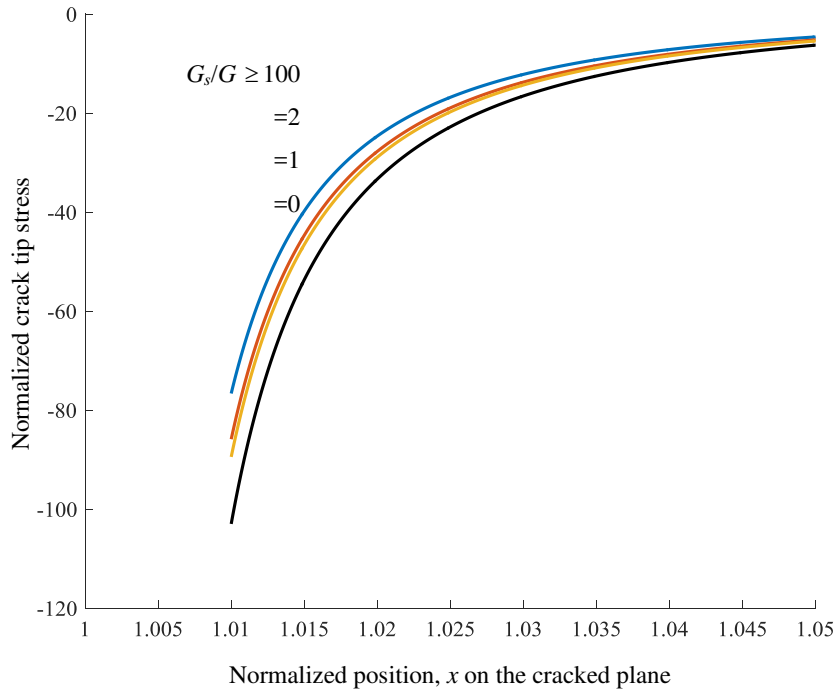


Figure 7. Normalized stress $\tau_y(x, 0)/p_0$ near the right crack tip in a in a film on a substrate of different stiffness for $h_1 = h_2 = 0.2a$, $l = 0.2a$, and $l_s = 2l$.

stress intensity factor K_{III} according to

$$lK_{III}(a) = \lim_{x \rightarrow a^+} 2\sqrt{2\pi(x-a)}(x-a)\tau_y(x, 0), \tag{28a}$$

$$lK_{III}(-a) = \lim_{x \rightarrow -a^-} 2\sqrt{2\pi(x+a)}(x+a)\tau_y(x, 0), \tag{28b}$$

and obtained the expressions as follows:

$$K_{III}(a) = \sqrt{\pi a} \frac{1}{2} \frac{l}{a} G \sum_{m=1}^{\infty} (m+1)A_m, \tag{29a}$$

$$K_{III}(-a) = \sqrt{\pi a} \frac{1}{2} \frac{l}{a} G \sum_{m=1}^{\infty} (-1)^m (m+1)A_m. \tag{29b}$$

The results of generalized stress intensity factor at the right crack tip, normalized with $K_0 = p_0\sqrt{\pi a}$, as functions of gradient parameters are plotted in Figure 8 for various values of the substrate stiffness. The gradient parameters for the strain gradient layer and the substrate layer are same. It is observed that the magnitude of the normalized stress intensity factor reduces with the stiffness of the substrate material. Also observed is that the magnitude of the normalized stress intensity factor decreases with the gradient parameter. The same tendency has been observed by Paulino et al. [2003] and Karimipour and Fotuhi [2017].

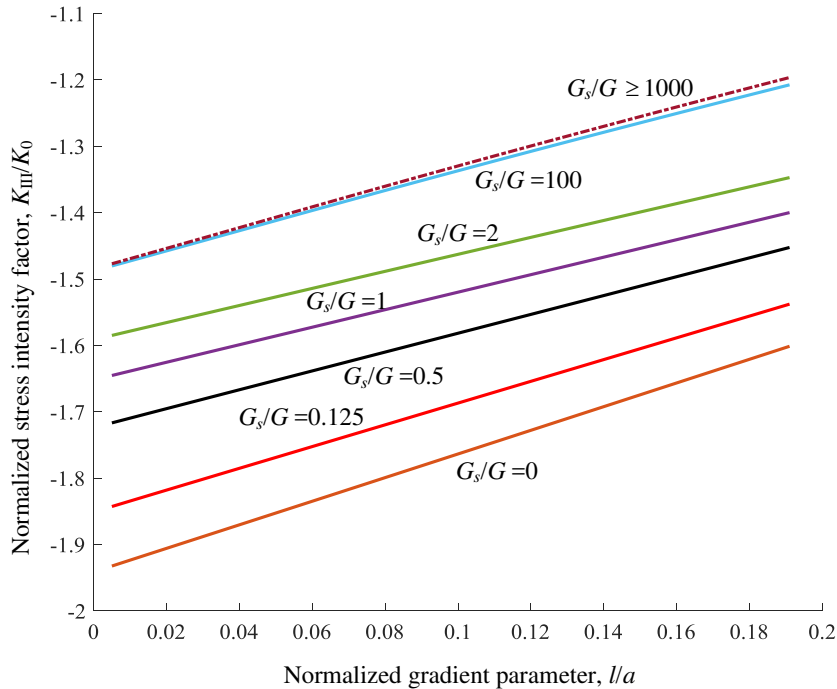


Figure 8. Normalized generalized stress intensity factor at the right crack tip for $h_1 = h_2 = 0.2a$ and $l_s = l$ where $K_0 = p_0\sqrt{\pi a}$. Due to symmetry, K_{III} at the left crack tip is opposite to these at the right crack tip.

5. Conclusion

A crack in a strain gradient layer on a substrate under anti-plane deformation has been studied. Both volumetric and surface strain gradient material constants are taken into consideration. The crack is parallel to the layer surface but is at any location in the strain gradient layer. The problem is governed by the solution of a hypersingular integral equation. It is found that when the gradient parameters are very small, results from the current strain gradient analysis reduce to the corresponding solutions of conventional linear fracture mechanics. Influences of strain gradient parameters, layer thickness and substrate stiffness have been conducted and are found to be very different from those of the conventional linear elastic fracture mechanics solutions.

Acknowledgements

This research was supported by the National Science Foundation of China (Project No. 11502101, 11672084, 11372086), Research Innovation Foundation of Jinling Institute of Technology (Project No. jit-b-201515), and the Research Innovation Fund of Shenzhen City (Project No. JCYJ20170413104256729).

Appendix

The following formulas [Paulino et al. 2003; Chan et al. 2008] have been used in deriving the hypersingular integral equations:

$$\frac{1}{\pi} \int_{-1}^1 \frac{U_m(r) \sqrt{1-r^2}}{(r-x)} dr = \begin{cases} -T_{m+1}(x), & m \geq 0, |x| < 1 \\ -[x - \frac{|x|}{x} \sqrt{x^2-1}]^{m+1}, & m \geq 0, |x| > 1 \end{cases}, \quad (\text{A1})$$

$$\frac{1}{\pi} \int_{-1}^1 \frac{U_m(r) \sqrt{1-r^2}}{(r-x)^3} dr = \begin{cases} \frac{1}{[4(1-x^2)]} [(m^2+m) U_{m+1}(x) - (m^2+3m+2) U_{m-1}(x)], & m \geq 1, |x| < 1 \\ -\frac{1}{2}(m+1) [x - \frac{|x|}{x} \sqrt{x^2-1}]^{m-1} \left[m \left(1 - \frac{|x|}{\sqrt{x^2-1}}\right)^2 + \frac{[x - \frac{|x|}{x} \sqrt{x^2-1}]}{(x^2-1)^{3/2}} \right], & m \geq 0, |x| > 1 \end{cases}. \quad (\text{A2})$$

References

- [Aifantis 2011] E. C. Aifantis, “A note on gradient elasticity and nonsingular crack fields”, *J. Mech. Behav. Mater* **20** (2011), 103–105.
- [Aifantis 2016] E. C. Aifantis, “Chapter 1: Internal length gradient (ILG) material mechanics across scales and disciplines”, pp. 1–110 in *Advances in applied mechanics*, vol. 49, edited by S. P. A. Bordas and D. S. Balint, Elsevier, 2016.
- [Benvenuti and Simone 2013] E. Benvenuti and A. Simone, “One-dimensional nonlocal and gradient elasticity: closed-form solution and size effect”, *Mech. Res. Commun.* **48** (2013), 46–51.
- [Chan et al. 2003] Y.-S. Chan, A. C. Fannjiang, and H. Glaucio, “Integral equations with hypersingular kernels—theory and applications to fracture mechanics”, *Int. J. Eng. Sci.* **41**:7 (2003), 683–720.
- [Chan et al. 2008] Y.-S. Chan, G. H. Paulino, and A. C. Fannjiang, “Gradient elasticity theory for mode III fracture in functionally graded materials—part II: crack parallel to the material gradation”, *J. Appl. Mech. (ASME)* **75** (2008), 061015.
- [Exadaktylos 1998] G. Exadaktylos, “Gradient elasticity with surface energy: mode-I crack problem”, *Int. J. Solids Struct.* **35**:5-6 (1998), 421–456.
- [Exadaktylos and Vardoulakis 2001] G. E. Exadaktylos and I. Vardoulakis, “Microstructure in linear elasticity and scale effects: a reconsideration of basic rock mechanics and rock fracture mechanics”, *Tectonophys.* **335**:1-2 (2001), 81–109.
- [Exadaktylos et al. 1996] G. Exadaktylos, I. Vardoulakis, and E. Aifantis, “Cracks in gradient elastic bodies with surface energy”, *Int. J. Fract.* **79** (1996), 107–119.
- [Fannjiang et al. 2002] A. C. Fannjiang, G. H. Paulino, and Y.-S. Chan, “Strain gradient elasticity for antiplane shear cracks: a hypersingular integrodifferential equation approach”, *SIAM J. Appl. Math.* **62**:3 (2002), 1066–1091.
- [Fleck et al. 1994] N. A. Fleck, G. M. Muller, M. F. Ashby, and J. W. Hutchinson, “Strain gradient plasticity: theory and experiment”, *Acta Metall. Mater.* **42**:2 (1994), 475–487.
- [Giannakopoulos and Stamoulis 2007] A. E. Giannakopoulos and K. Stamoulis, “Structural analysis of gradient elastic components”, *Int. J. Solids Struct.* **44**:10 (2007), 3440–3451.
- [Grosskreutz and Mcneilt 1969] J. C. Grosskreutz and M. B. Mcneilt, “The fracture of surface coatings on a strained substrate”, *J. Appl. Phys.* **40** (1969), 355–359.
- [Hutchinson et al. 1987] J. W. Hutchinson, M. E. Mear, and J. R. Rice, “Crack paralleling an interface between dissimilar materials”, *J. Appl. Mech. (ASME)* **54**:4 (1987), 828–832.
- [Karimipour and Fotuhi 2017] I. Karimipour and A. R. Fotuhi, “Anti-plane analysis of an infinite plane with multiple cracks based on strain gradient theory”, *Acta Mech.* **228**:5 (2017), 1793–1817.
- [Kiang et al. 1998] C.-H. Kiang, M. Endo, P. M. Ajayan, G. Dresselhaus, and M. S. Dresselhaus, “Size effects in carbon nanotubes”, *Phys. Rev. Lett.* **81**:9 (1998), 1869–1872. also in arXiv:cond-mat/9811046.

- [Kim and Nairn 2000] S.-R. Kim and J. A. Nairn, "Fracture mechanics analysis of coating/substrate systems: part I: analysis of tensile and bending experiments", *Eng. Fract. Mech.* **65**:5 (2000), 573–593.
- [Koiter 1964] W. Koiter, "Couple stresses in the theory of elasticity, I & II", *Philos. Trans. Royal Soc. B* **67** (1964), 17–44.
- [Lam et al. 2003] D. C. C. Lam, F. Yang, A. C. M. Chong, J. Wang, and P. Tong, "Experiments and theory in strain gradient elasticity", *J. Mech. Phys. Solids* **51**:8 (2003), 1477–1508.
- [Ma and Clarke 1995] Q. Ma and D. R. Clarke, "Size dependent hardness of silver single crystals", *J. Mater. Res.* **10**:4 (1995), 853–863.
- [McElhaney et al. 1998] K. W. McElhaney, J. J. Vlassak, and W. D. Nix, "Determination of indenter tip geometry and indentation contact area for depth-sensing indentation experiments", *J. Mater. Res.* **13**:5 (1998), 1300–1306.
- [McFarland and Colton 2005] A. W. McFarland and J. S. Colton, "Role of material microstructure in plate stiffness with relevance to microcantilever sensors", *J. Micromech. Microeng.* **15**:5 (2005), 1060–1067.
- [Mindlin 1965] R. D. Mindlin, "Second gradient of strain and surface-tension in linear elasticity", *Int. J. Solids Struct.* **1**:4 (1965), 417–438.
- [Mindlin and Eshel 1968] R. D. Mindlin and N. N. Eshel, "On first strain-gradient theories in linear elasticity", *Int. J. Solids Struct.* **4**:1 (1968), 109–124.
- [Mindlin and Tiersten 1962] R. Mindlin and H. Tiersten, "Effects of couple-stresses in linear elasticity", *Arch. Ration. Mech. Anal.* **11**:1 (1962), 415–448.
- [Mousavi and Aifantis 2005] S. M. Mousavi and E. Aifantis, "A note on dislocation-based mode III gradient elastic fracture mechanics", *J. Mech. Behav. Mater.* **24**:3-4 (2005), 115–119.
- [Nix 1989] W. D. Nix, "Mechanical properties of thin films", *Metall. Mater. Trans. A* **20** (1989), 2217.
- [Paulino et al. 2003] G. H. Paulino, A. C. Fannjiang, and Y.-S. Chan, "Gradient elasticity theory for mode III fracture in functionally graded materials—part I: crack perpendicular to the material gradation", *J. Appl. Mech. (ASME)* **70**:4 (2003), 531–542.
- [Piccolroaz et al. 2012] A. Piccolroaz, G. Mishuris, and E. Radi, "Mode III interfacial crack in the presence of couple-stress elastic materials", *Eng. Fract. Mech.* **80** (2012), 60–71.
- [Poole et al. 1996] W. J. Poole, M. F. Ashby, and N. A. Fleck, "Micro-hardness of annealed and work-hardened copper polycrystals", *Scr. Mater.* **34**:4 (1996), 559–564.
- [Qiu et al. 2018] Y. Qiu, H. Wu, J. Wang, J. Lou, Z. Zhang, A. Liu, and G. Chai, "The enhanced piezoelectricity in compositionally graded ferroelectric thin films under electric field: a role of flexoelectric effect", *J. Appl. Phys.* **123**:8 (2018), 084103.
- [Schulze and Erdogan 1998] G. W. Schulze and F. Erdogan, "Periodic cracking of elastic coatings", *Int. J. Solids Struct.* **35**:28-29 (1998), 3615–3634.
- [Shi et al. 2014] M. Shi, H. Wu, L. Li, and G. Chai, "Calculation of stress intensity factors for functionally graded materials by using the weight functions derived by the virtual crack extension technique", *Int. J. Mech. Mater. Des.* **10**:1 (2014), 65–77.
- [Stelmashenko et al. 1993] N. A. Stelmashenko, M. G. Walls, L. M. Brown, and Y. V. Milman, "Microindentations on W and Mo oriented single crystals: an STM study", *Acta Metall. Mater.* **41**:10 (1993), 2855–2865.
- [Stolken 1997] J. S. Stolken, *The role of oxygen in nickel-sapphire interface fracture*, Ph.D. dissertation, University of California, Santa Barbara, 1997.
- [Toupin 1962] R. A. Toupin, "Elastic materials with couple-stresses", *Arch. Ration. Mech. Anal.* **11**:1 (1962), 385–414.
- [Vardoulakis et al. 1996] I. Vardoulakis, G. Exadaktylos, and E. Aifantis, "Gradient elasticity with surface energy: mode-III crack problem", *Int. J. Solids Struct.* **33**:30 (1996), 4531–4559.
- [Wu et al. 2016a] H. Wu, L. Li, G. Chai, F. Song, and T. Kitamura, "Three-dimensional thermal weight function method for the interface crack problems in bimaterial structures under a transient thermal loading", *J. Therm. Stresses* **39**:4 (2016), 371–385.
- [Wu et al. 2016b] H. Wu, X. Ma, Z. Zhang, J. Zhu, J. Wang, and G. Chai, "Dielectric tunability of vertically aligned ferroelectric-metal oxide nanocomposite films controlled by out-of-plane misfit strain", *J. Appl. Phys.* **119**:15 (2016), 154102.
- [Zhang et al. 1998] L. Zhang, Y. Huang, Y. J. Chen, and K. C. Hwang, "The mode III full-field solution in elastic materials with strain gradient effects", *Int. J. Fract.* **92**:4 (1998), 325–348.

Received 18 Jun 2018. Revised 3 Oct 2018. Accepted 3 Oct 2018.

JINE LI: lijine@jit.edu.cn

School of Architectural Engineering, Jinling Institute of Technology, China

BAOLIN WANG: wangbl2001@hotmail.com

School of Science, Harbin Institute of Technology (Shenzhen), China

JOURNAL OF MECHANICS OF MATERIALS AND STRUCTURES

msp.org/jomms

Founded by Charles R. Steele and Marie-Louise Steele

EDITORIAL BOARD

ADAIR R. AGUIAR	University of São Paulo at São Carlos, Brazil
KATIA BERTOLDI	Harvard University, USA
DAVIDE BIGONI	University of Trento, Italy
MAENGHYO CHO	Seoul National University, Korea
HUILING DUAN	Beijing University
YIBIN FU	Keele University, UK
IWONA JASIUK	University of Illinois at Urbana-Champaign, USA
DENNIS KOCHMANN	ETH Zurich
MITSUTOSHI KURODA	Yamagata University, Japan
CHEE W. LIM	City University of Hong Kong
ZISHUN LIU	Xi'an Jiaotong University, China
THOMAS J. PENCE	Michigan State University, USA
GIANNI ROYER-CARFAGNI	Università degli studi di Parma, Italy
DAVID STEIGMANN	University of California at Berkeley, USA
PAUL STEINMANN	Friedrich-Alexander-Universität Erlangen-Nürnberg, Germany
KENJIRO TERADA	Tohoku University, Japan

ADVISORY BOARD

J. P. CARTER	University of Sydney, Australia
D. H. HODGES	Georgia Institute of Technology, USA
J. HUTCHINSON	Harvard University, USA
D. PAMPLONA	Universidade Católica do Rio de Janeiro, Brazil
M. B. RUBIN	Technion, Haifa, Israel

PRODUCTION production@msp.org

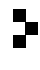
SILVIO LEVY Scientific Editor

See msp.org/jomms for submission guidelines.

JoMMS (ISSN 1559-3959) at Mathematical Sciences Publishers, 798 Evans Hall #6840, c/o University of California, Berkeley, CA 94720-3840, is published in 10 issues a year. The subscription price for 2018 is US \$615/year for the electronic version, and \$775/year (+\$60, if shipping outside the US) for print and electronic. Subscriptions, requests for back issues, and changes of address should be sent to MSP.

JoMMS peer-review and production is managed by EditFLOW® from Mathematical Sciences Publishers.

PUBLISHED BY

 **mathematical sciences publishers**
nonprofit scientific publishing

<http://msp.org/>

© 2018 Mathematical Sciences Publishers

Journal of Mechanics of Materials and Structures

Volume 13, No. 4

July 2018

-
- Prediction of springback and residual stress of a beam/plate subjected to three-point bending** **QUANG KHOA DANG, PEI-LUN CHANG, SHIH-KANG KUO and DUNG-AN WANG** **421**
- Characterization of CNT properties using space-frame structure** **MUHAMMAD ARIF and JACOB MUTHU** **443**
- Analytical approach to the problem of an auxetic layer under a spatially periodic load** **HENRYK KAMIŃSKI and PAWEŁ FRITZKOWSKI** **463**
- Stability and nonplanar postbuckling behavior of current-carrying microwires in a longitudinal magnetic field** **YUANZHUO HONG, LIN WANG and HU-LIANG DAI** **481**
- Three-dimensional Trefftz computational grains for the micromechanical modeling of heterogeneous media with coated spherical inclusions** **GUANNAN WANG, LEITING DONG, JUNBO WANG and SATYA N. ATLURI** **505**
- Uniform stress resultants inside two nonelliptical inhomogeneities in isotropic laminated plates** **XU WANG, LIANG CHEN and PETER SCHIAVONE** **531**
- An analytical solution for heat flux distribution of cylindrically orthotropic fiber reinforced composites with surface effect** **JUNHUA XIAO, YAOLING XU and FUCHENG ZHANG** **543**
- Strain gradient fracture of a mode III crack in an elastic layer on a substrate** **JINE LI and BAOLIN WANG** **555**
- Growth-induced instabilities of an elastic film on a viscoelastic substrate: analytical solution and computational approach via eigenvalue analysis** **IMAN VALIZADEH, PAUL STEINMANN and ALI JAVILI** **571**
- Application of the hybrid complex variable method to the analysis of a crack at a piezoelectric-metal interface** **VOLODYMYR GOVORUKHA and MARC KAMLAH** **587**



1559-3959(2018)13:4;1-Y